

pubs.acs.org/Macromolecules Article

# Orthogonal Atom Transfer Radical Polymerization and Reversible Addition—Fragmentation Chain Transfer Polymerization for Controlled Polymer Architectures

Bing Niu, Li Zhang, and Jianbo Tan\*



**Cite This:** *Macromolecules* 2024, 57, 9766–9778



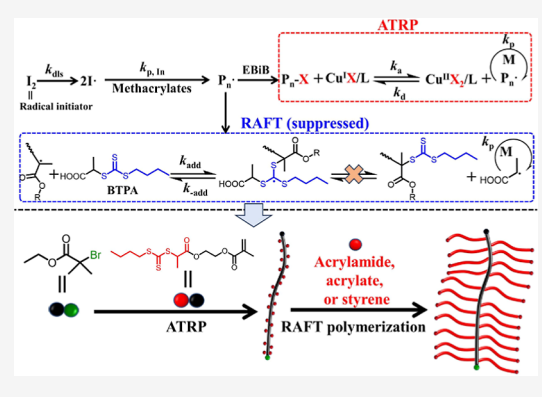
**ACCESS** I

III Metrics & More

Article Recommendations

Supporting Information

ABSTRACT: Here, we report an orthogonal atom transfer radical polymerization (ATRP) and reversible addition—fragmentation chain transfer (RAFT) polymerization approach by selecting a suitable RAFT agent. Reverse ATRP of poly(ethylene glycol) methyl ether methacrylate using ethyl 2-bromoisobutyrate was performed in the presence of 2-(n-butyltrithiocarbonate)propionic acid (BTPA). Size exclusion chromatography and UV—vis spectroscopy confirmed that BTPA remained inert under reverse ATRP conditions. The effect of the structure of the RAFT agent on the orthogonal ATRP—RAFT polymerization was then investigated in detail, demonstrating the importance of the leaving R-group of the RAFT agent. This approach was then used to copolymerize and homopolymerize a RAFT chain transfer monomer (CTM), 2-(2-(n-butyltrithiocarbonate)propionate)ethyl methacrylate, under ATRP conditions with the trithiocarbonate group on the CTM unit being unreacted.



RAFT solution polymerization and RAFT dispersion polymerization were then performed to synthesize graft and bottlebrush copolymers. Upon RAFT dispersion polymerization, graft copolymer assemblies were also obtained, and the effect of the distribution of solvophobic side chains on graft copolymer assemblies was investigated. This approach not only provides a facile route for the rational synthesis of well-defined polymers with controlled architectures but also offers new mechanistic insights into ATRP and RAFT polymerization.

#### INTRODUCTION

Over the past 20 years or so, reversible deactivation radical polymerization (RDRP) has become one of the most versatile polymerization techniques that enables the rational synthesis of well-defined polymers with precise molecular weight, low dispersity, diverse chemical functionality, and controlled polymer architecture. 1-9 Among various RDRP techniques, atom transfer radical polymerization (ATRP)<sup>10</sup> and reversible addition-fragmentation chain transfer (RAFT) polymerization 11 have attracted increasing attention due to their distinct advantages such as excellent controllability, tolerance to various functional groups and solvents, and mild reaction conditions. For a copper (Cu)-catalyzed ATRP, the Cu complex in its lower oxidation state reacts with an alkyl halide initiator to generate propagating radicals and an oxidized Cu complex coordinated to a halide. The deactivating Cu-halide complex can further react with propagating radicals to regenerate the dormant polymer chains and the original Cu complex.<sup>12</sup> For a typical RAFT polymerization, a thiocarbonylthio compound is usually used and can react with propagating radicals to generate an intermediate radical, which can further form a new propagating radical and a dormant thiocarbonythio-capped polymer chain through the fragmentation of the weak carbon-sulfide bond. 13 In both ATRP and RAFT polymerization, the formation of polymer chains with narrow molecular weight distributions is facilitated by rapid and reversible exchange between dormant and active chain ends. While ATRP reduces radical—radical termination, RAFT outcompetes termination through a reversible chain transfer process, ensuring controlled polymer growth.<sup>14</sup> Upon the completion of polymerization, most polymer chains retain their halide or thiocarbonyl end-groups that can further chain extend to form block copolymers.<sup>15,16</sup>

One emerging direction of this research area is the development of orthogonal RDRP methodologies that can access unique copolymer compositions such as bottlebrush polymers. Recently, a variety of orthogonal RAFT polymerizations have been developed by several research groups. For example, Xu, Boyer, and co-workers explored a novel wavelength selective photoinduced electron/energy transfer RAFT (PET-RAFT) polymerization using two different RAFT agents and two different photocatalysts, allowing selective

Received: August 4, 2024
Revised: September 21, 2024
Accepted: September 26, 2024
Published: October 4, 2024





Scheme 1. (a) Proposed Mechanism for the Combined ATRP-RAFT Polymerization of Methacrylic Monomers; (b) Chemical Structures of ATRP Initiator, Ligand, and RAFT Agents Used in the Present Study

control for orthogonal RAFT polymerizations. In their study, they demonstrated that the dithiobenzoate RAFT agent was activated and the trithiocarbonate RAFT agent was inactivated under red light irradiation, while the trithiocarbonate RAFT agent could be reactivated under green light irradiation. You and co-workers<sup>20</sup> reported an orthogonal radical and cationic RAFT polymerization using two distinct RAFT agents. Selective cationic RAFT polymerization of a RAFT inimer bearing trithiocarbonate remains inactivated during the cationic RAFT polymerization. A second monomer can be grafted from the pendant trithiocarbonate groups via radical RAFT polymerization to form well-defined bottlebrush polymers. Matyjaszewski and co-workers<sup>21</sup> developed a wavelength selective photoiniferter RAFT polymerization of methacrylic monomers using two RAFT agents with different leaving R-groups. Under photoiniferter conditions (green light irradiation), only one RAFT agent was activated, while the other RAFT agent was inactivated. Through green light-activated photoiniferter RAFT (co)polymerization of a methacrylic RAFT inimer and the subsequently blue-light-activated photoiniferter RAFT polymerization of an acrylamide monomer, well-defined comblike and bottlebrush polymer were successfully obtained.

Despite some significant achievements having been made in orthogonal RAFT polymerizations, these methodologies would lead to the formation of polymers with a RAFT end-group. This defect in the polymer structure would lead to the growth of a side chain at the chain end and therefore poor performance for some specific applications. As an alternative, orthogonal ATRP—RAFT polymerization is an attractive strategy to overcome this issue since the polymer backbone can be synthesized based on ATRP and the halide end-group is inactivated under RAFT polymerization conditions. However, radicals generated during ATRP may also react with the RAFT agent that would lead to the undesired crossover. As a result, the orthogonal ATRP—RAFT polymerization always requires the implementation of RAFT polymerization first and then ATRP. This strategy

limits the synthesis of RAFT polymers with various structures that can be used for the preparation of polymer assemblies by RAFT-mediated polymerization-induced self-assembly (RAFT-PISA).<sup>31–38</sup> Therefore, it is highly desirable to develop orthogonal ATRP-RAFT polymerization that can perform ATRP first and then RAFT polymerization.

In this study, we develop an orthogonal ATRP-RAFT polymerization for the facile synthesis of graft and bottlebrush copolymers. In contrast to previous work that requires the implementation of RAFT polymerization first, our study focuses on a reverse sequence that can perform ATRP first and then RAFT polymerization by selecting a suitable RAFT agent. The RAFT agent is inactivated during ATRP of methacrylic monomers that can be further activated via conventional RAFT polymerization of acrylamide, acrylate, or styrene (St). We also performed ATRP of a methacrylic RAFT chain transfer monomer (CTM) in the first step before switching to the second step to enable the RAFT polymerization of acrylamide and St, allowing the preparation of graft and bottlebrush copolymers. Multifunctional macro-RAFT agents with different structures synthesized by orthogonal ATRP-RAFT polymerization were also used to mediate RAFT dispersion polymerization, demonstrating the advantages of orthogonal ATRP-RAFT polymerization.

# ■ RESULTS AND DISCUSSION

Investigation of the Reactivity of RAFT Agents during Reverse ATRP of the Methacrylic Monomer. The overarching goal of the present study is to explore a RAFT polymerization that can remain dormant during ATRP and can reactivate via the subsequent polymerization. In our previous work, <sup>39,40</sup> taking advantage of different RAFT controllability of two RAFT agents toward methacrylic monomers, we demonstrated that 2-(*n*-butyltrithiocarbonate)propionic acid (BTPA) was inactivated during photoinitiated RAFT polymerization of

Table 1. Summary of Polymers Synthesized by Reverse ATRP of PEGMA in the Presence of Different Types and Amounts of the RAFT Agent

entry	[PEGMA]/[EBiB]/[RAFT agent]	RAFT agent	monover conversion (%) <sup>a</sup>	DP	$M_{\rm n} \left({\rm kg/mol}\right)^{b}$	$M_{\rm w}/M_{\rm n}^{}$
1	15/1/0	none	93.2	14.1	8.70	1.11
2	15/1/2	ETPA	91.7	13.8	8.85	1.11
3	15/1/2	BTPA	93.5	14.0	9.03	1.08
4	15/1/2	DTPA	91.7	13.7	8.91	1.10
5	15/1/1	BDTC	94.4	14.3	7.84	1.13
6	15/1/2	BDTC	94.5	14.3	7.73	1.13
7	15/1/1	DDMAT	95.9	14.4	7.20	1.17
8	15/1/2	DDMAT	95.0	14.2	7.39	1.15
9	15/1/1	CDPA	93.9	14.1	4.90	1.15
10	15/1/2	CDPA	90.4	13.6	3.62	1.13

<sup>a</sup>The monomer conversion was determined by <sup>1</sup>H NMR spectroscopy.  $^bM_{\rm n}$  and  $M_{\rm w}/M_{\rm n}$  were checked by SEC against linear poly(methyl methacrylate) standards.

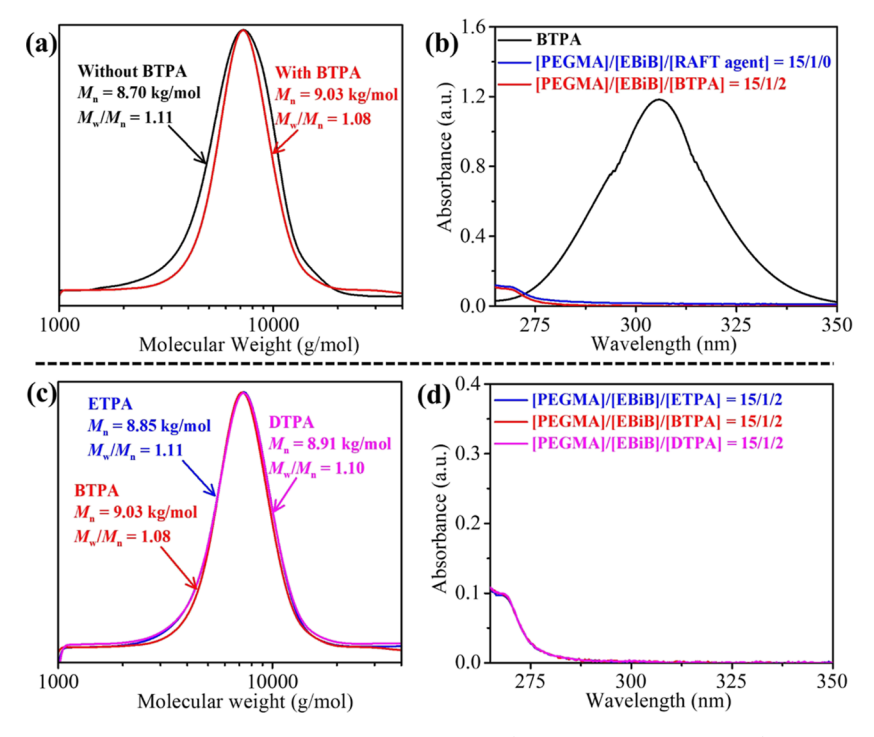


Figure 1. (a) SEC traces of polymers synthesized by reverse ATRP of PEGMA ([PEGMA]/[EBiB] = 15/1) in the absence or presence of BTPA ([PEGMA]/[EBiB]/[BTPA] = 15/1/2). (b) UV—vis spectra of BTPA and purified polymers synthesized by reverse ATRP of PEGMA ([PEGMA]/[EBiB] = 15/1) in the absence or presence of BTPA ([PEGMA]/[EBiB]/[BTPA] = 15/1/2). (c) SEC traces of polymers synthesized by reverse ATRP of PEGMA in the presence of ETPA, BTPA, or DPTA ([PEGMA]/[EBiB]/[RAFT agent] = 15/1/2). (d) UV—vis spectra of purified polymers synthesized by reverse ATRP of PEGMA in the presence of ETPA, BTPA, or DPTA ([PEGMA]/[EBiB]/[RAFT agent] = 15/1/2).

methacrylic monomers using 4-cyano-4-(ethylthiocarbonothioylthio)pentanoic acid (CEPA) as the RAFT agent and sodium phenyl 2,4,6-trimethylbenzoylphosphinate (SPTP) as the photoinitiator. This phenomenon can be explained by the fact that methacrylyl propagating radicals are prone to react with CEPA to generate new radicals, while the reaction pathway of methacrylyl propagating radicals with BTPA is greatly suppressed. Inspired by these results, we assumed that RAFT agents with poor RAFT controllability toward methacrylic monomers could also remain dormant during a reverse ATRP of methacrylic monomers using a traditional initiator. As shown in Scheme 1a, the reaction pathway of methacrylyl propagating radicals should be dominated by the ATRP process. In the meantime, the possible formation of intermediate adduct radicals between methacrylyl-propagating radicals and the RAFT agent eventually fragments back to the original species.

An initial Cu-catalyzed reverse ATRP of poly(ethylene glycol) methyl ether methacrylate (PEGMA,  $M_n = 475$  g/mol) was performed at 70 °C for 12 h using 2,2-azobissobutyronitri (AIBN) as the initiator in the presence of ethyl 2bromoisobutyrate (EBiB), CuCl<sub>2</sub>, and tris(2-pyridylmethyl)amine (TPMA) ([PEGMA]/[EBiB] = 15/1). The polymerization resulted in 93.2% monomer conversion (Table 1, entry 1). Symmetrical size exclusion chromatography (SEC) trace with a narrow molecular weight distribution  $(M_w/M_p = 1.11)$ was observed for this polymer (black line in Figure 1a). The reverse Cu-catalyzed ATRP of PEGMA was then performed under the same conditions in the presence of BTPA ([EBiB]/ [BTPA] = 1/2). After 12 h of polymerization, a high monomer conversion (93.5%) was still achieved (Table 1, entry 3). More importantly, it was found that the SEC trace of the polymer synthesized in the presence of BTPA was almost identical with

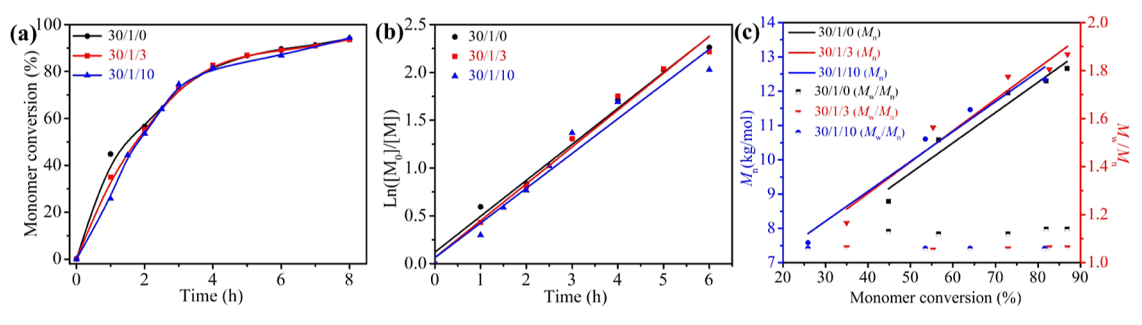


Figure 2. (a) Polymerization kinetics of reverse ATRP of PEGMA in the absence or presence of BTPA with different [PEGMA]/[EBiB]/[BTPA] ratios. (b) Plots of  $\ln([M]_0/[M])$  vs reaction time for reverse ATRP of PEGMA in the absence or presence of BTPA with different [PEGMA]/[EBiB]/[BTPA] ratios. (c) Evolution of number-average molecular weight  $(M_n)$  and molecular weight distribution  $(M_w/M_n)$  with monomer conversion for reverse ATRP of PEGMA in the absence or presence of BTPA with different [PEGMA]/[EBiB]/[BTPA] ratios.

the polymer synthesized in the absence of BTPA (Figure 1a). These polymers were purified by several precipitations in petroleum ether/ethyl ether (5/5, v/v) and further analyzed by UV—vis spectroscopy. As shown in Figure 1b, no absorption was observed at 310 nm (characteristic absorption of trithiocarbonate) for these polymers, suggesting that no trithiocarbonate group was incorporated into the polymer structure. The supernatant of the polymerization was also concentrated and characterized by  $^1$ H NMR spectroscopy (Figure S1), which clearly displayed the characteristic signal of unreacted BTPA at  $\delta$  = 4.80 ppm (—CH in the adjacent trithiocarbonate group). These results suggest that BTPA did not participate in the Cucatalyzed reverse ATRP of PEGMA when using EBiB as the ATRP initiator and TPMA as the ligand.

Inspired by these initial findings, we assumed that the reactivity of RAFT agents during reverse ATRP of PEGMA should mainly rely on the structure of the RAFT agent and, more precisely, on the structure of the Z-group and leaving R-group. Control experiments were then performed to understand the structure—property relationship of the reactivity of RAFT agents in the reverse ATRP of PEGMA. Conventional RAFT polymerization of PEGMA was first performed using BTPA without the addition of EBiB, CuCl<sub>2</sub>, and TPMA. In these cases, high monomer conversions and broad molecular weight distributions were observed (Figure S2). This can be attributed to the mismatch of the propagating methacrylyl radical (tertiary carbon) and the reinitiating radical from BTPA (secondary carbon) as well as the poor  $\beta$ -scission of the carbon–sulfide bond (Scheme 1a). Reverse ATRP of PEGMA was also performed in the presence of 2-(n-ethyltrithiocarbonate)propionic acid (ETPA), BTPA (the same as Figure 1a) or 2-(n-dodecyltrithiocarbonate)propionic acid (DTPA) with the [PEGMA]/[EBiB]/[RAFT agent] ratio of 15/1/2. These RAFT agents share the same leaving R-group but with different alkyl Z-groups. High PEGMA conversions (≥91.7%) were observed in all cases as confirmed by <sup>1</sup>H NMR spectroscopy (Table 1, entry 2-4). Figure 1c shows that these SEC traces almost overlap, suggesting that these RAFT agents also did not participate in the ATRP process. Moreover, it was demonstrated that the Z-groups of these RAFT agents had no influence on the reactivity of the RAFT agent during reverse ATRP of PEGMA. UV-vis spectra of the purified polymers indicated the absence of signal at 310 nm characteristic of the trithiocarbonate group (Figure 1d). Furthermore, <sup>1</sup>H NMR analysis confirmed the absence of the trithiocarbonate group in the polymer structure (Figure S3).

Polymerization kinetics of reverse ATRP of PEGMA in the absence ([PEGMA]/[EBiB] = 30/1) or in the presence of BTPA ([PEGMA]/[EBiB]/[BTPA] = 30/1/3 or 30/1/10) was then investigated. As shown in Figure 2a,b, similar polymerization behaviors were observed in all cases, and over 90% monomer conversions were achieved within 7 h of polymerization. The presence of BTPA in the reaction mixture gave a comparable propagation rate constant to a reaction mixture without BTPA. Increasing the amount of BTPA led to a slightly lower polymerization rate for PEGMA, which should be attributed to the presence of an additional reaction pathway for PPEGMA radicals. This pathway would lead to the possible generation of intermediate adduct radicals between PPEGMA propagating radicals and BTPA which will fragment back to their original species (Scheme 1a), but this will reduce the overall radical concentration in the polymerization system and therefore slower polymerization. Purified polymers obtained during the kinetic studies were also analyzed by SEC (Figure 2c). Comparable molecular weights with narrow molecular weight distributions were observed, which further confirms that BTPA did not participate in the ATRP process with propagating PPEGMA radicals. In each case, a linear evolution of  $M_n$  with monomer conversion was also observed, which is one of the typical characteristics of controlled/"living" polymerization. 41 It should be noted that polymers synthesized in the presence of BTPA exhibit narrower molecular weight distributions than the polymers synthesized in the absence of BTPA. This may be attributed to the relatively low radical concentration in the polymerization system with BTPA that can reduce the possibility of radical-radical termination.

We then further investigated the effect of leaving the R-group structure on the reactivity of the RAFT agent during reverse ATRP of PEGMA. Reverse ATRP of PEGMA was then performed in the presence of benzyl dodecyl trithiocarbonate (BDTC), S-1-dodecyl-S'-( $\alpha$ , $\alpha$ '-dimethyl- $\alpha$ "-acetic acid) trithiocarbonate (DDMAT), or 4-cyano-4-[(dodecylsulfanylthiocarbonyl)sulfanyl] pentanoic acid (CDPA) with the [PEGMA]/[EBiB]/[RAFT] ratio of 15/1/1 or 15/1/2 (Table 1, entry 5-10). These RAFT agents share the same Z-group  $(C_{12})$  but with different leaving R-groups. Compared with DTPA that has a carboxyl-stabilized secondary carbon R-group, DDMAT has a carboxyl-stabilized tertiary carbon R-group that should have a higher transfer coefficient. Due to the similar structure of the leaving R-group of DDMAT with the methacrylyl propagating radical, DDMAT can partially control the RAFT polymerization of methacrylic monomers. 42,43 The leaving R-group of BDTC (benzyl group) has a

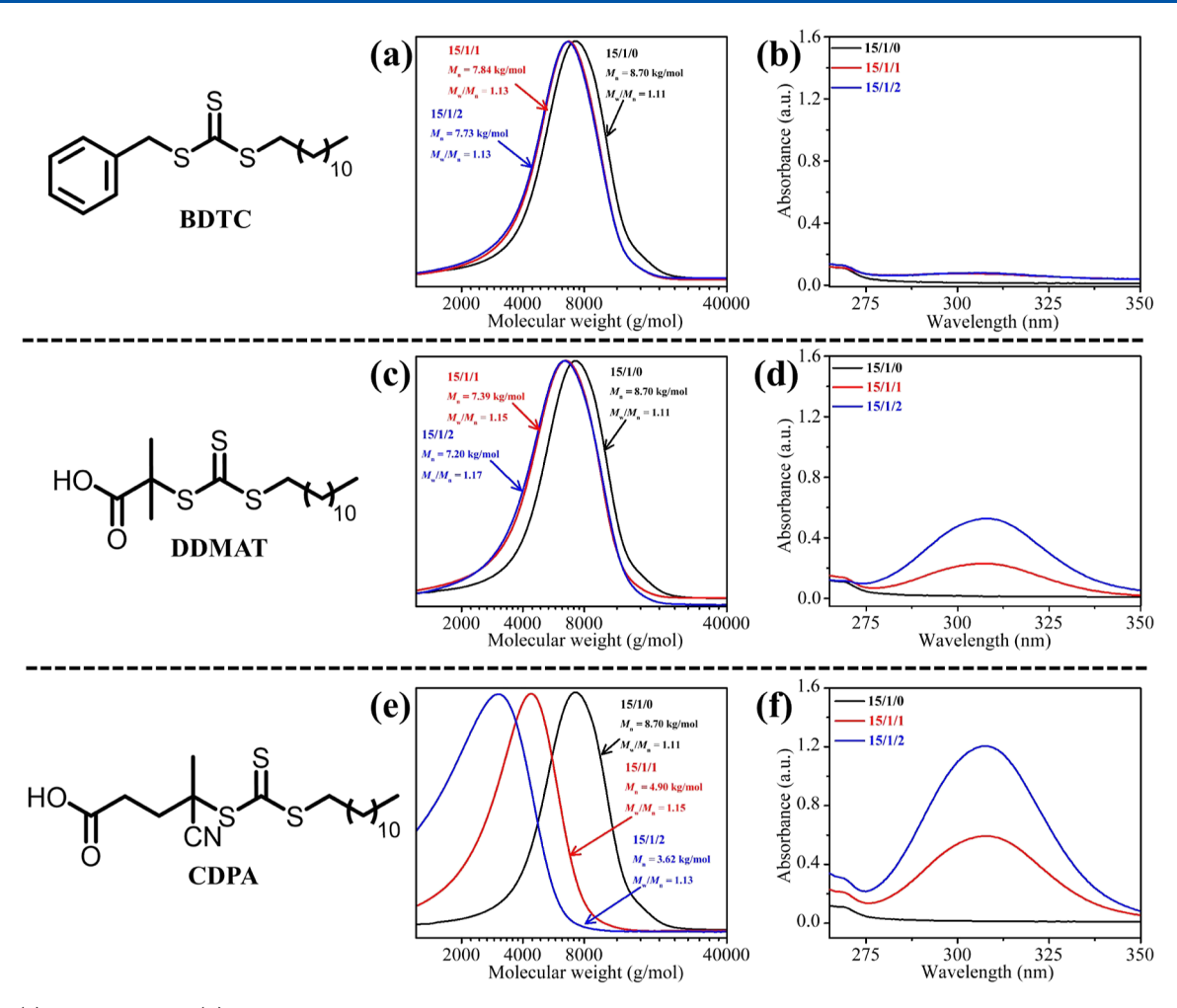
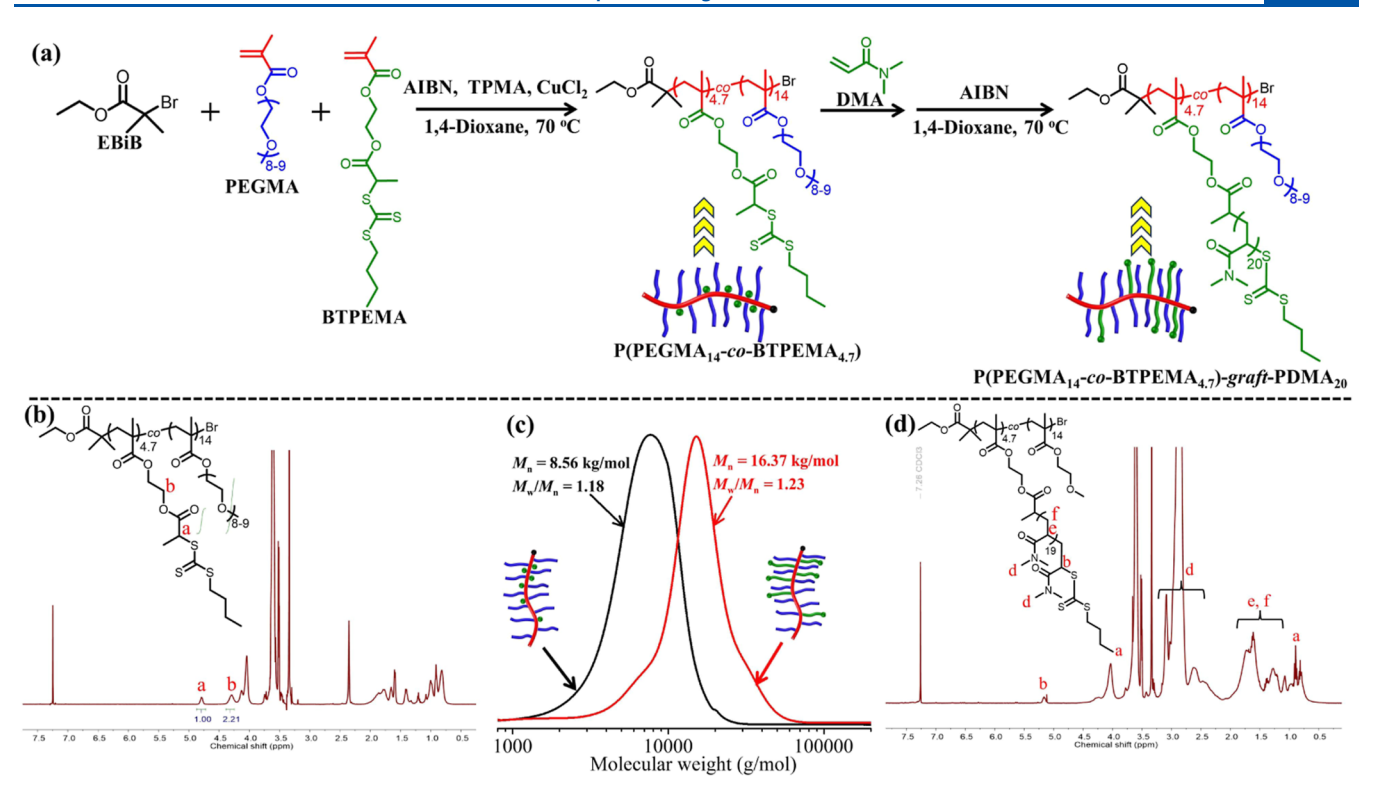


Figure 3. (a) SEC traces and (b) UV—vis spectra of polymers synthesized by reverse ATRP of PEGMA in the absence of presence of BDTC with different [PEGMA]/[EBiB]/[BDTC] ratios. (c) SEC traces and (d) UV—vis spectra of polymers synthesized by reverse ATRP of PEGMA in the absence or presence of DDMAT with different [PEGMA]/[EBiB]/[DDMAT] ratios. (e) SEC traces and (f) UV—vis spectra of polymers synthesized by reverse ATRP of PEGMA in the absence or presence of CDPA with different [PEGMA]/[EBiB]/[CDPA] ratios. Note: In each case, a polymer concentration of 1.0 mg/mL was employed for the UV—vis spectroscopy characterization.

lower transfer coefficient than the leaving R-group of DDMAT,<sup>5</sup> and it is expected that BDTC should exhibit poorer RAFT controllability toward methacrylic monomers. Figure 3 shows SEC traces of the polymers obtained in the presence of different RAFT agents. In the presence of BDTC, the SEC trace shifted slightly to lower molecular weight (Figure 3a), and the  $M_n$  value was decreased slightly from 8.70 kg/mol ([EBiB]/[BDTC] = 1/0) to 7.84 kg/mol ([EBiB]/[BDTC] = 1/1) and 7.73 kg/mol ([EBiB]/[BDTC] = 1/2). This is due to the partial participation of BDTC during reverse ATRP of PEGMA. This can be further confirmed by the UV-vis spectra of the purified polymers. As shown in Figure 3b, a weak absorption signal at 310 nm was observed for each polymer, which is the characteristic absorption of trithiocarbonate group. A large amount of unreacted BDTC was separated during the purification of the obtained polymers (Figure S4). Similar observations were also observed in reverse ATRP of PEGMA in the presence of DDMAT. Compared with the case of BDTC, it was found that more DDMAT participated during reverse ATRP of PEGMA (Figure 3c). For example, the decrease of  $M_n$  value was more obvious in the presence of DDMAT (e.g., 8.70 kg/mol for [EBiB]/[DDMAT] = 1/0 to 7.39 kg/mol [EBiB]/[DDMAT] =1/1). A noticeable amount of unreacted DDMAT was also

found in the solution (Figure S5). Compared with the polymers synthesized in the presence of BDTC (Figure 3b), a stronger UV-vis absorption at 310 nm was observed for the polymers synthesized in the presence of DDMAT (Figure 3d). In contrast, CDPA is a well-known RAFT agent that exhibits excellent RAFT controllability toward methacrylic monomers due to the high transfer efficient of the (4-cyanopentanoicacid) radical Rgroup. 44 Figure 3e shows SEC traces of polymers obtained by the reverse ATRP of PEGMA in the presence of CDPA with the [PEGMA]/[EBiB]/[CDPA] ratio of 15/1/1 or 15/1/2. It was found that the SEC trace shifted significantly to lower molecular weight with decreasing [EBiB]/[CDPA] ratio. Moreover, the obtained polymers exhibited strong absorption at the wavelength of 310 nm (Figure 3f). These results suggest that CDPA can efficiently participate in the reverse ATRP of PEGMA and that the polymerization of PEGMA should undergo a mixed mechanism of ATRP and RAFT polymerization. <sup>1</sup>H NMR analysis also verified the presence of a CDPA end group in the formed polymer (Figure S6).

Synthesis of Graft and Bottlebrush Copolymers by Orthogonal ATRP-RAFT Polymerization. With the established orthogonal ATRP-RAFT polymerization, we then intend to expand this method for the synthesis of complex



**Figure 4.** (a) Schematic illustration for the synthesis of P(PEGMA<sub>14</sub>-co-BTPEMA<sub>4,7</sub>) by reverse ATRP of PEGMA and BTPEMA using EBiB and the subsequent grafting of PDMA chains through conventional RAFT polymerization of DMA at 70 °C. (b) ¹H NMR spectrum of P(PEGMA<sub>14</sub>-co-BTPEMA<sub>4,7</sub>). (c) SEC traces of P(PEGMA<sub>14</sub>-co-BTPEMA<sub>4,7</sub>) (black line) and P(PEGMA<sub>14</sub>-co-BTPEMA<sub>4,7</sub>)-graft-PDMA<sub>20</sub> (red line). (d) ¹H NMR spectrum of P(PEGMA<sub>14</sub>-co-BTPEMA<sub>4,7</sub>)-graft-PDMA<sub>20</sub>.

architectures, including graft and bottlebrush copolymers. A RAFT-based CTM was first synthesized by linking BTPA and hydroxyethyl methacrylate via esterification, denoted as 2-(2-(nbutyltrithiocarbonate)propionate)ethyl methacrylate (BTPE-MA, Figure S9). Reverse ATRP of PEGMA and BTPEMA was then performed with a [PEGMA]/[EBiB]/[BTPEMA] ratio of 15/1/5 (Figure 4a). The obtained polymer (P-(PEGMA<sub>14</sub>-co-BTPEMA<sub>4.7</sub>), as determined by <sup>1</sup>H NMR analysis), exhibited a narrow molecular weight distribution  $(M_{\rm w}/M_{\rm n}=1.18)$  with a  $M_{\rm n}$  value of 8.56 kg/mol (black line in Figure 4c). Further analysis of the purified polymer with <sup>1</sup>H NMR spectroscopy indicated the successful incorporation of BTPEMA into the polymer structure (Figure 4b). Moreover, the presence of a proton signal at 4.80 ppm confirmed that the pendant trithiocarbonate group was inactivated during reverse ATRP. The purified P(PEGMA<sub>14</sub>-co-BTPEMA<sub>4.7</sub>) was then grafted with N,N-dimethylacrylamide (DMA) through a conventional thermally RAFT polymerization (Figure 4a). A graft copolymer (P(PEGMA<sub>14</sub>-co-BTPEMA<sub>4.7</sub>)-graft-PDMA<sub>20</sub>) was synthesized with a relatively narrow molecular weight distribution  $(M_w/M_n = 1.23)$  (red line in Figure 4c). It should be noted that copolymerization with fewer than 6 units of BPTMA would result in more than 5% of the polymers without the incorporation of BPTMA by random distribution. 45 Therefore, a small low-molecular-weight peak was also observed in the SEC trace after the polymerization of DMA. <sup>1</sup>H NMR spectrum of the purified polymer revealed grafting of PDMA from  $P(PEGMA_{14}-co-BTPEMA_{4,7})$  with the appearance of a  $-CH_3$ peak at 2.80-3.00 ppm (peak d in Figure 4d).

To further demonstrate the versatility of this approach, we then attempted to synthesize bottlebrush copolymers through a grafting-from approach (Figure 5a). Backbones of bottlebrush

polymers were synthesized by reverse ATRP of BTPEMA at 70  $^{\circ}$ C for 12 h at different [BTPEMA]/[EBiB] ratios. The average degree of polymerization (DP) of each polymer chain was determined by <sup>1</sup>H NMR spectroscopy. Figure 5b shows SEC traces of PBTPEMA with different DPs. Relatively narrow molecular weight distribution  $(M_w/M_n \le 1.28)$  was observed in each case and the number-average molecular weight increased linearly with the average DP of PBTPEMA (Figure 5c). <sup>1</sup>H NMR spectrum of PBTPEMA232 revealed that the integra of signal at 3.30 ppm (peak c in Figure 5d) is twice that of signal at 4.80 ppm (peak a in Figure 5d), confirming the trithiocarbonate group remained intact during reverse ATRP of BTPEMA. It should be noted that this approach is also versatile to traditional ATRP (Figure S10). As a proof-of-concept experiment, PBTPEMA<sub>97</sub> was then grafted with polystyrene (PSt) through a thermally initiated RAFT polymerization of St at 70 °C. The DP of PSt side chain was also determined by the St conversion and the resulting bottlebrush polymer (PBTPEMA97-graft-PSt<sub>6</sub>) exhibited a relatively narrow molecular weight distribution  $(M_{\rm w}/M_{\rm n}=1.33)$  (Figure 5e). Figure S11 shows the <sup>1</sup>H NMR spectrum of PBTPEMA<sub>97</sub>-graft-PSt<sub>6</sub> and the complete disappearance of the signal at 4.80 ppm after RAFT polymerization of St, suggesting that all pendant trithiocarbonate groups involved the grafting reaction. The architecture of bottlebrush polymers can be further controlled by using a trifunctional ATRP initiator. Using the similar approach, a three-arm star-like bottlebrush polymer was also successfully synthesized (Figures S12 and 13).

Graft Copolymer Assemblies Prepared via RAFT Dispersion Polymerization Using Multifunctional Macro-RAFT Agents. Over the past ten years or so, polymerization-induced self-assembly via RAFT dispersion

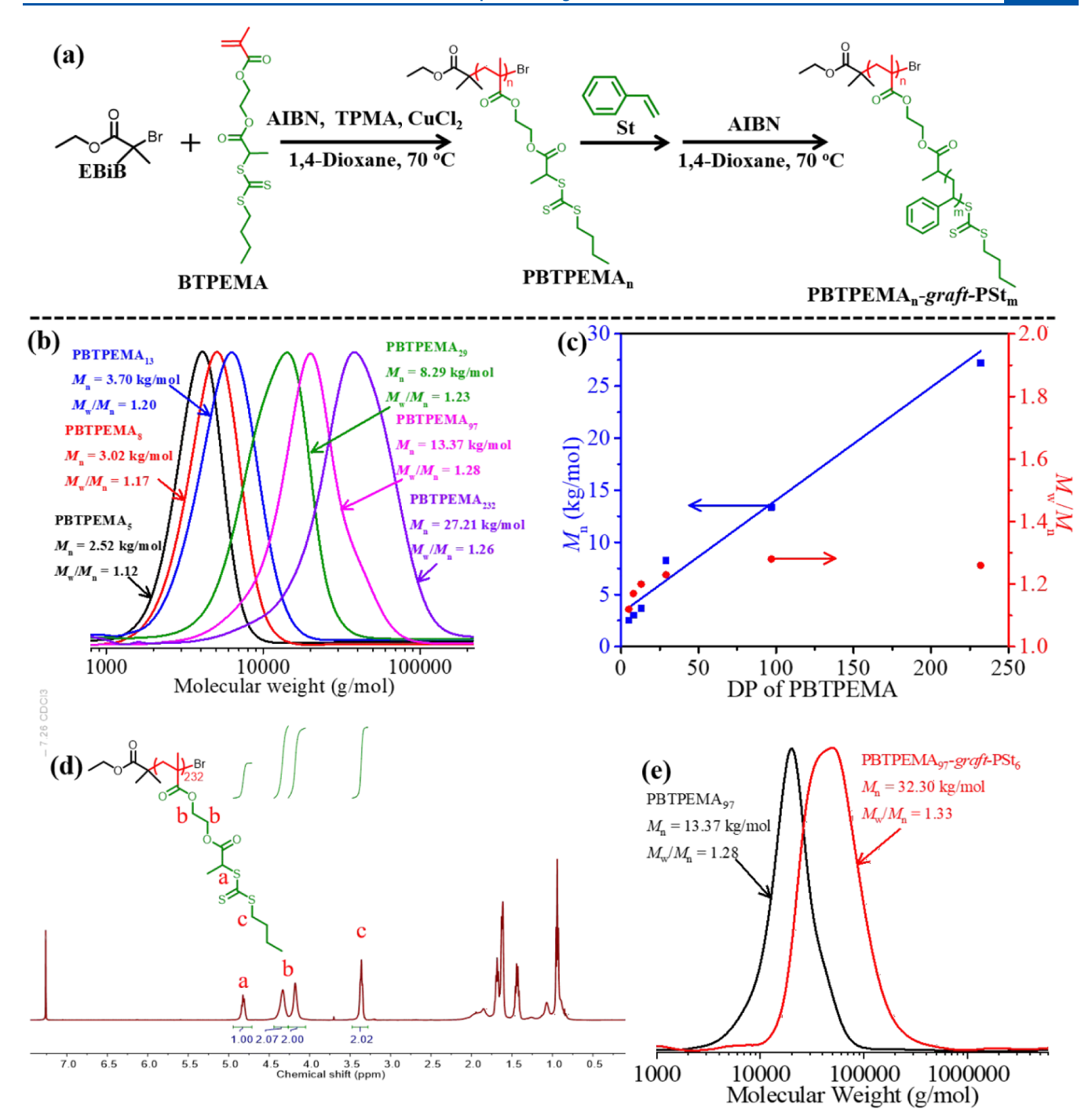


**Figure 5.** (a) Schematic illustration for the synthesis of PBTPEMA<sub>n</sub> by reverse ATRP of BTPEMA and the subsequent grafting of PSt side chains through conventional RAFT polymerization. (b) SEC traces of PBTPEMA<sub>n</sub> (n = 5, 8, 13, 29, 97, 232) synthesized by reverse ATRP of BTPEMA. (c) Evolution of  $M_n$  and  $M_w/M_n$  with DP of PBTPEMA. (d) <sup>1</sup>H NMR spectrum of PBTPEMA<sub>232</sub>. (e) SEC traces of PBTPEMA<sub>97</sub> and PBTPEMA<sub>97</sub>-graft-PSt<sub>6</sub>.

polymerization has become a powerful technique for the rational synthesis of polymer assemblies with various morphologies. 46–60 Recently, we and others have demonstrated that the architecture of macromolecular RAFT (macro-RAFT) agents played an important role in the PISA process and the morphology of polymer assemblies. 61–66 The established orthogonal ATRP—RAFT polymerization enables the synthesis of multifunctional macro-RAFT agents with diverse architectures. In this section, we also explored the potential of

orthogonal ATRP-RAFT polymerization in PISA for the preparation of graft copolymer assemblies.

First, a series of multifunctional macro-RAFT agents were synthesized by a two-step reverse ATRP of PEGMA and BTPEMA ([PEGMA]/[BTPEMA]/[EBiB] = 20/4/1). BTPE-MA was added into the polymerization at intermediate PEGMA conversion that can control the distribution of RAFT groups in the polymer structure (Scheme 2). Table 2 shows recipes for the macro-RAFT agents synthesized by the two-step reverse ATRP of PEGMA and BTPEMA. <sup>1</sup>H NMR analysis confirmed that

Scheme 2. Schematic Illustration for the Synthesis of Multifunctional Macro-RAFT Agents with Different RAFT Group Distributions by a Two-Step Reverse ATRP of PEGMA and BTPEMA

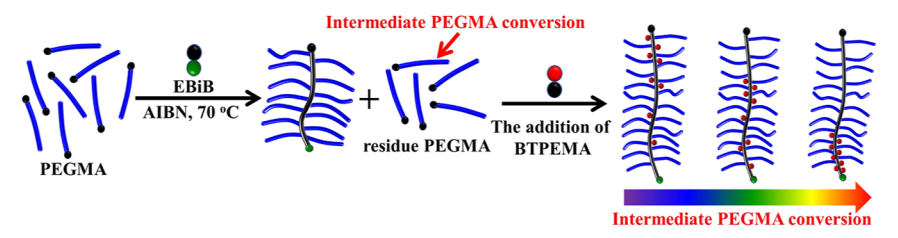
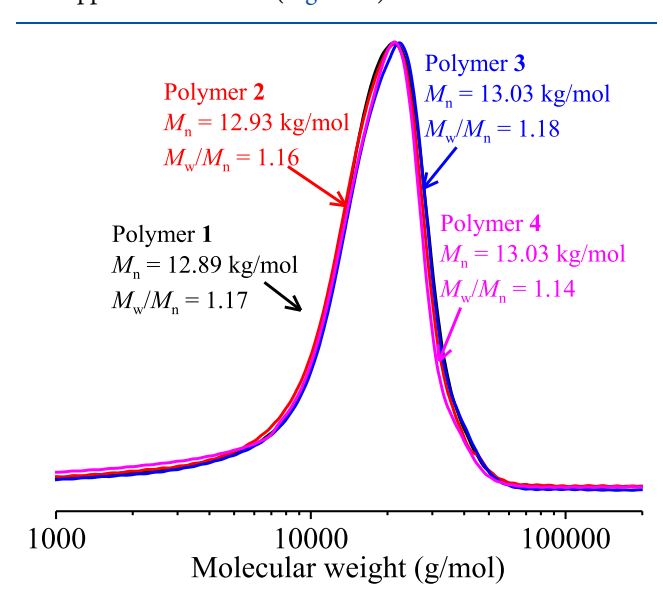


Table 2. Summary for the Synthesis of Multifunctional Macro-RAFT Agents by a Two-Step Reverse ATRP of PEGMA and BTPEMA

polymer	[PEGMA]/[BTPEMA]/[EBiB]	intermediate PEGMA conversion (%) <sup>a</sup>	overall PEGMA conversion (%) <sup>a</sup>	overall BTPEMA conversion (%) <sup>a</sup>	$\frac{M_{\mathrm{n}}}{(\mathrm{kg/mol})^{b}}$	$M_{\rm w}/M_{ m n}^{}$
1	20/4/1	0	97.8	98.5	12.89	1.17
2	20/4/1	62.2	99.3	95.0	12.93	1.16
3	20/4/1	82.6	98.9	98.5	13.03	1.18
4	20/4/1	94.1	99.2	95.0	13.03	1.14

<sup>&</sup>quot;Monomer conversions were determined by  $^1$ H NMR spectroscopy.  $^bM_{\rm n}$  and  $M_{\rm w}/M_{\rm n}$  were determined by SEC against poly(methyl methacrylate) standards.

high overall PEGMA and BTPEMA conversions were achieved in all cases. These macro-RAFT agents share similar molecular weights and chemical compositions, as evidenced by the overlapped SEC traces (Figure 6). When the intermediate



**Figure 6.** SEC traces of multifunctional macro-RAFT agents synthesized by a two-step reverse ATRP of PEGMA and BTPEMA.

PEGMA conversion is 0%, the RAFT groups should distribute randomly along the polymer backbone. On increasing the intermediate PEGMA conversion, the RAFT groups should taper from the bromide end-group (Scheme 2). With these macro-RAFT agents in hand, one could investigate the effect of the solvophobic side chain distribution on the morphology of graft copolymer assemblies under PISA conditions.

RAFT dispersion polymerizations of St (20% w/w) were then performed in methanol/water (8/2, w/w) by using these multifunctional macro-RAFT agents with different [St]/[macro-RAFT] ratios. High monomer conversions were achieved in all cases, as confirmed by <sup>1</sup>H NMR analysis. Moreover, a coagulum-free dispersion was obtained in each case.

Upon RAFT dispersion polymerization, graft copolymers with PSt side chains were obtained. The structure of graft copolymers is determined by the structure of macro-RAFT agents (Figure 7a). For example, the PSt side chains would distribute randomly within the graft copolymer when using polymer 1 as the macro-RAFT agent; while the PSt side chain would mainly distribute at the bromide end-group when using polymer 4 as the macro-RAFT agent. Figure S14 shows SEC traces of graft copolymers obtained by RAFT dispersion polymerization of St using these multifunctional macro-RAFT agents with a [St]/[macro-RAFT] ratio of 100. Multimodal SEC traces were observed in all cases. This is because the formed polymers should be a mixture of graft copolymers with different number of side chains. Figure 7b-q shows transmission electron microscopy (TEM) images of the formed graft copolymer assemblies prepared by the RAFT dispersion polymerization of St using these macro-RAFT agents. When polymer 1 was used as the macro-RAFT agent, spheres mixed with vesicles were observed at the [St]/ [macro-RAFT] ratio of 100 (Figure 7b). A pure vesicular morphology was observed at the [St]/[macro-RAFT] ratio of 150 or 200 (Figure 7c,d). Further increasing the [St]/[macro-RAFT ratio to 250 led to the formation of large compound vesicles (Figure 7e). In contrast, mixed morphologies of vesicles and spheres were observed at all investigated [St]/[macro-RAFT] ratios when polymer 2 was used as the macro-RAFT agent (Figure 7f-i). When polymer 3 or polymer 4 was used as the macro-RAFT agent, pure spheres were obtained at the [St]/ [macro-RAFT] ratio of 100 (Figure 7j,n), and mixed morphologies were observed when the [St]/[macro-RAFT] ratio was 150 or higher (Figure 7k-m,o-q). These results suggest that higher-order morphologies are favor when the PSt side chains distributed along the polymer backbone, which can be attributed to the enhanced fusion between micelles (a key step for the morphological evolution). In contrast, the possibility of fusion between micelles is reduced when the PSt side chains grow mainly at one chain end of the graft copolymers and therefore lower-order morphologies are favor.

We then further explored this method to synthesize star-like graft copolymer assemblies by replacing EBiB with a trifunctional ATRP initiator (TMP-Br<sub>3</sub>). As shown in Scheme 3a, a

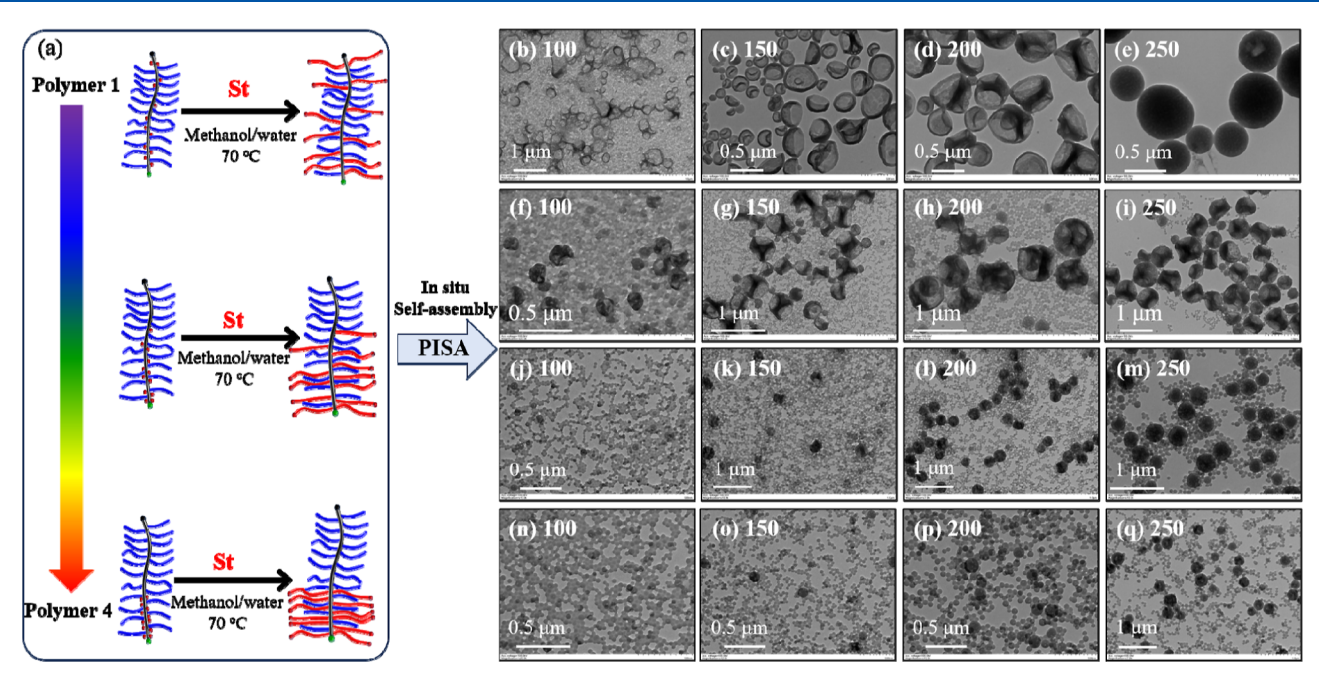
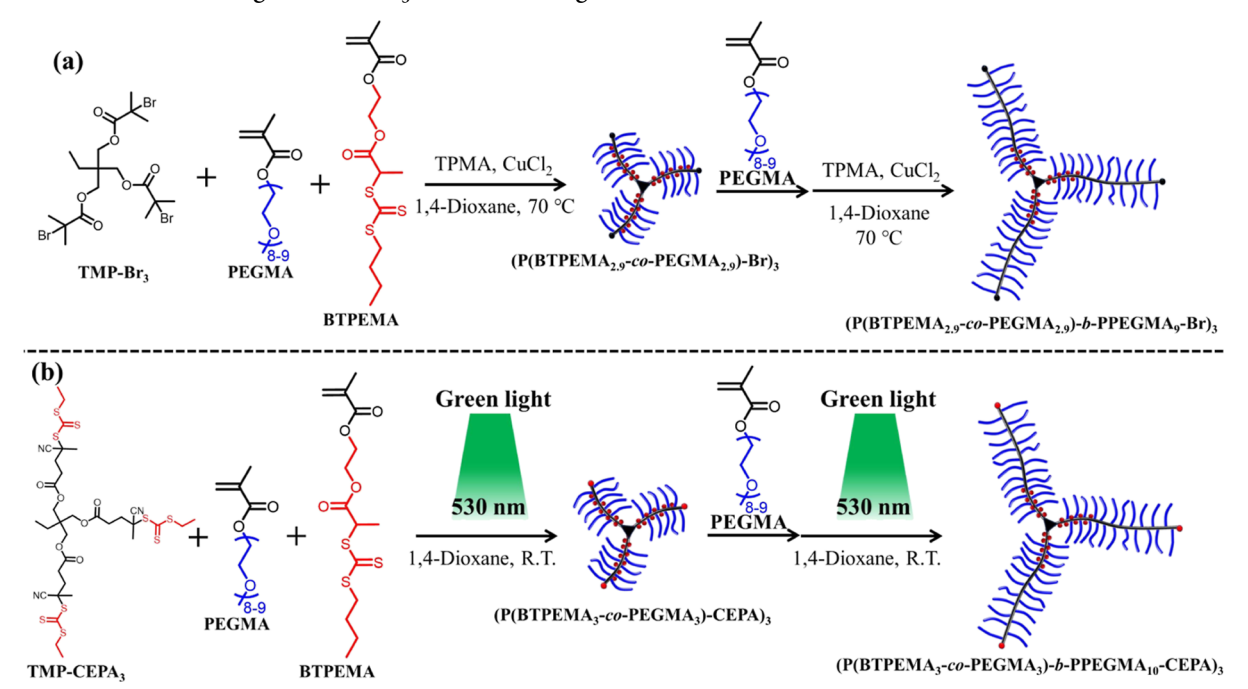


Figure 7. (a) Schematic illustration for the synthesis of graft copolymers by RAFT dispersion polymerization of St in methanol/water using the multifunctional macro-RAFT agents. (b–e) TEM images of graft copolymer assemblies prepared by RAFT dispersion polymerization of St using polymer 1 as the macro-RAFT agent with different [St]/[macro-RAFT] ratios. (f–i) TEM images of graft copolymer assemblies prepared by RAFT dispersion polymerization of St using polymer 2 as the macro-RAFT agent with different [St]/[macro-RAFT] ratios. (j–m) TEM images of graft copolymer assemblies prepared by RAFT dispersion polymerization of St using polymer 3 as the macro-RAFT agent with different [St]/[macro-RAFT] ratios. (n–q) TEM images of graft copolymer assemblies prepared by RAFT dispersion polymerization of St using polymer 4 as the macro-RAFT agent with different [St]/[macro-RAFT] ratios.

Scheme 3. (a) Schematic Illustration for the Synthesis of 3-Arm Star-like Multifunctional Macro-RAFT Agent by a Two-Step Reverse ATRP of PEGMA and BTPEMA Using TMP-Br<sub>3</sub> as the ATRP Initiator; (b) Schematic Illustration for the Synthesis of 3-Arm Star-like Multifunctional Macro-RAFT Agent by a Two-Step Green Light-Activated Photoiniferter RAFT Polymerization of PEGMA and BTPEMA Using TMP-CEPA<sub>3</sub> as the RAFT Agent



star-like macro-RAFT agent was synthesized by the two-step reverse ATRP of PEGMA and BTPEMA, denoted as (P(BTPEMA<sub>2.9</sub>-co-PEGMA<sub>2.9</sub>)-b-PPEGMA<sub>9</sub>-Br)<sub>3</sub>. As a control experiment, a two-step green light-activated photoiniferter

RAFT polymerization was also employed to synthesize a starlike multifunctional macro-RAFT agent with a similar structure (Scheme 3b), denoted as (P(BTPEMA<sub>3</sub>-co-PEGMA<sub>3</sub>)-b-PPEGMA<sub>10</sub>-CEPA)<sub>3</sub>. These two macro-RAFT agents were

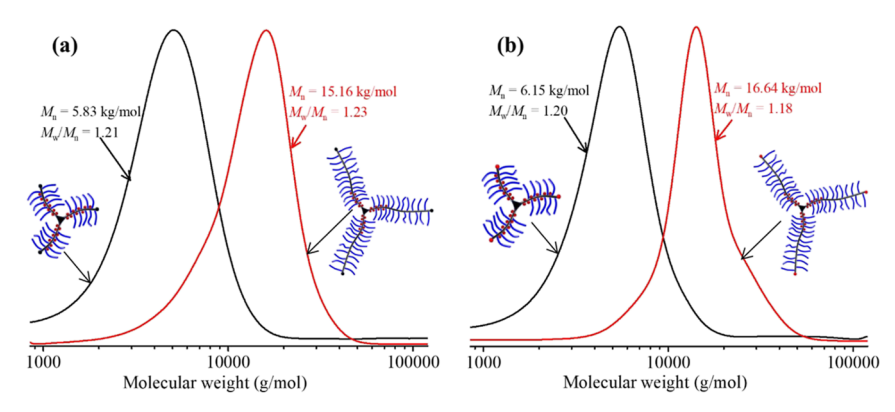


**Figure 8.** (a) SEC traces of (P(BTPEMA<sub>2.9</sub>-co-PEGMA<sub>2.9</sub>)-Br)<sub>3</sub> and (P(BTPEMA<sub>2.9</sub>-co-PEGMA<sub>2.9</sub>)-b-PPEGMA<sub>9</sub>-Br)<sub>3</sub> synthesized by reverse ATRP of PEGMA and BTPEMA. (b) SEC traces of (P(BTPEMA<sub>3</sub>-co-PEGMA<sub>3</sub>)-CEPA)<sub>3</sub> and (P(BTPEMA<sub>3</sub>-co-PEGMA<sub>3</sub>)-b-PPEGMA<sub>10</sub>-CEPA)<sub>3</sub> synthesized by green light-activated photoiniferter RAFT polymerization of PEGMA and BTPEMA.

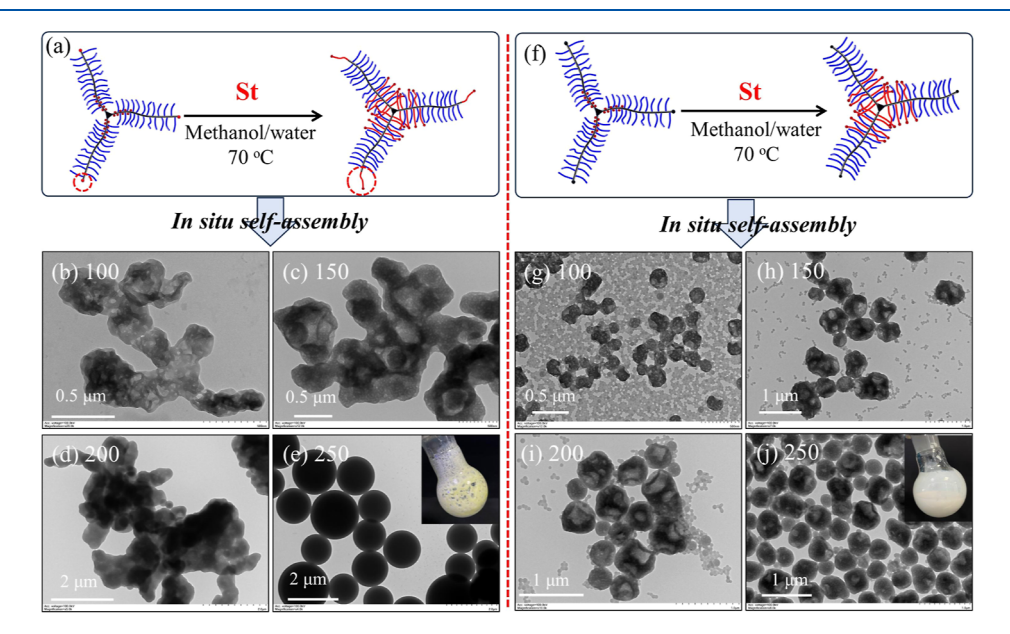


Figure 9. (a) Schematic illustration for the synthesis of star-like graft copolymers by RAFT dispersion polymerization of St using (P(BTPEMA<sub>3</sub>-co-PEGMA<sub>3</sub>)-b-PPEGMA<sub>10</sub>-CEPA)<sub>3</sub> as the macro-RAFT agent. (b—e) TEM images of graft copolymer assemblies prepared by RAFT dispersion polymerization of St using (P(BTPEMA<sub>3</sub>-co-PEGMA<sub>3</sub>)-b-PPEGMA<sub>10</sub>-CEPA)<sub>3</sub> as the macro-RAFT agent with different [St]/[macro-RAFT] ratios. (f) Schematic illustration for the synthesis of star-like graft copolymers by RAFT dispersion polymerization of St using (P(BTPEMA<sub>2,9</sub>-co-PEGMA<sub>2,9</sub>)-b-PPEGMA<sub>9</sub>-Br)<sub>3</sub> as the macro-RAFT agent. (g—j) TEM images of graft copolymer assemblies prepared by RAFT dispersion polymerization of St using (P(BTPEMA<sub>2,9</sub>-co-PEGMA<sub>2,9</sub>)-b-PPEGMA<sub>3</sub>-Br)<sub>3</sub> as the macro-RAFT agent with different [St]/[macro-RAFT] ratios.

analyzed by SEC (Figure 8), and comparable molecular weights and narrow molecular weight distributions were observed. These two macro-RAFT agents were then used to mediate RAFT dispersion polymerization of St (20% w/w) with different [St]/[macro-RAFT] ratios. It was found that the formed polymers cannot dissolve in THF for SEC analysis, which can be attributed to the occurrence of radical-radical termination in the core-forming block. When (P(BTPEMA<sub>3</sub>-co-PEGMA<sub>3</sub>)-b-PPEGMA<sub>10</sub>-CEPA)<sub>3</sub> was used as the macro-RAFT agent, large aggregates of polymer particles were observed at the [St]/ [macro-RAFT] ratio of 200 or lower (Figure 9b-d). When the [St]/[macro-RAFT] ratio reached 250, precipitation occurred during the polymerization (inset image in Figure 9e) and large spheres were observed for the dispersed part (Figure 9e). This should be attributed to the occurrence of bridging events between polymer particles because some PSt side chains always grow at the periphery of star graft copolymers (Figure 9a). This hypothesis can be supported by using (P(BTPEMA<sub>2.9</sub>-coPEGMA<sub>2.9</sub>)-b-PPEGMA<sub>9</sub>-Br)<sub>3</sub> as the macro-RAFT agent since the bromide end groups cannot be activated under RAFT dispersion polymerization conditions (Figure 9f). Colloidally stable dispersions were obtained in all cases, even the [St]/[macro-RAFT] ratio reached 250 (Figure 9g-j). Moreover, no aggregation was observed for the resulting polymer particles. Dynamic light scattering (DLS) data of these samples also verified the morphological difference (Figure S16). These results demonstrate that the orthogonal ATRP—RAFT polymerization offers new opportunities for the synthesis of well-defined polymers for some specific applications.

#### CONCLUSIONS

In summary, we have successfully developed an orthogonal ATRP–RAFT polymerization via careful selection of the leaving R-group of the RAFT agent. Unlike previous orthogonal ATRP–RAFT polymerization that RAFT polymerization has to be performed first to avoid undesired crossover, this work

provides a new orthogonal ATRP-RAFT polymerization that can perform ATRP first and then RAFT polymerization. The effect of the structure of the RAFT agent on the orthogonal ATRP-RAFT polymerization was investigated in detail. Copolymerization and homopolymerization of BTPEMA were performed via reverse ATRP with the trithiocarbonate group on the BTPEMA unit being unreacted. RAFT solution polymerization of DMA or St was then performed to generate welldefined graft and bottlebrush copolymers. Finally, RAFT dispersion polymerization of St was also employed to synthesize graft copolymers with different distributions of side chains and the assemblies. It was found that the distribution of solvophobic side chains of graft copolymers had a significant influence on the morphology of graft copolymer assemblies. This approach offers new opportunities for the synthesis of complex macromolecular architectures for some specific applications.

#### ASSOCIATED CONTENT

## **5** Supporting Information

The Supporting Information is available free of charge at https://pubs.acs.org/doi/10.1021/acs.macromol.4c01856.

Experimental details, materials, and methods; <sup>1</sup>H NMR spectra of concentrated supernatant of reversed ATRP of PEGMA; <sup>1</sup>H NMR spectra of polymers obtained by reversed ATRP of PEGMA; additional SEC traces of polymers prepared by RAFT or reverse ATRP; <sup>1</sup>H NMR spectra of BTPEMA, PBTPEMA<sub>97</sub>-graft-PSt<sub>6</sub>, TMP-Br<sub>3</sub>, TMP-CEPA<sub>3</sub>; SEC traces of graft copolymers; and DLS data of 3-arm graft copolymer nanoparticles (PDF)

## AUTHOR INFORMATION

## **Corresponding Author**

Jianbo Tan — Department of Polymeric Materials and Engineering, School of Materials and Energy, Guangdong University of Technology, Guangzhou 510006, China; Guangdong Provincial Key Laboratory of Functional Soft Condensed Matter, Guangzhou 510006, China; orcid.org/0000-0002-5635-7178; Email: tanjianbo@gdut.edu.cn

### **Authors**

Bing Niu – Department of Polymeric Materials and Engineering, School of Materials and Energy, Guangdong University of Technology, Guangzhou 510006, China

Li Zhang — Department of Polymeric Materials and Engineering, School of Materials and Energy, Guangdong University of Technology, Guangzhou 510006, China; Guangdong Provincial Key Laboratory of Functional Soft Condensed Matter, Guangzhou 510006, China

Complete contact information is available at: https://pubs.acs.org/10.1021/acs.macromol.4c01856

#### **Notes**

The authors declare no competing financial interest.

## ACKNOWLEDGMENTS

The authors acknowledge support from the National Natural Science Foundation of China (grants 52222301, 22171055), the Guangdong Natural Science Foundation for Distinguished Young Scholar (grant 2022B1515020078), and the Science and Technology Program of Guangzhou (grant 2024A04J2821). They would like to thank Wei Song of Analysis

and Test Center of Guangdong University of technology for DLS measurement.

#### REFERENCES

- (1) Corrigan, N.; Jung, K.; Moad, G.; Hawker, C. J.; Matyjaszewski, K.; Boyer, C. Reversible-Deactivation Radical Polymerization (Controlled/Living Radical Polymerization): From Discovery to Materials Design and Applications. *Prog. Polym. Sci.* **2020**, *111*, 101311.
- (2) Destarac, M. Industrial Development of Reversible-Deactivation Radical Polymerization: Is the Induction Period Over? *Polym. Chem.* **2018**, *9* (40), 4947–4967.
- (3) Nicolas, J.; Guillaneuf, Y.; Lefay, C.; Bertin, D.; Gigmes, D.; Charleux, B. Nitroxide-Mediated Polymerization. *Prog. Polym. Sci.* **2013**, 38 (1), 63–235.
- (4) Matyjaszewski, K. Atom Transfer Radical Polymerization (ATRP): Current Status and Future Perspectives. *Macromolecules* **2012**, 45 (10), 4015–4039.
- (5) Perrier, S. 50th Anniversary Perspective: RAFT Polymerization-A User Guide. *Macromolecules* **2017**, *50* (19), 7433–7447.
- (6) Hill, M. R.; Carmean, R. N.; Sumerlin, B. S. Expanding the Scope of RAFT Polymerization: Recent Advances and New Horizons. *Macromolecules* **2015**, 48 (16), 5459–5469.
- (7) Kamigaito, M.; Ando, T.; Sawamoto, M. Metal-Catalyzed Living Radical Polymerization. *Chem. Rev.* **2001**, *101* (12), 3689–3746.
- (8) Lin, D.-n.; Zhang, L.; Tan, J. Room-temperature Heterogeneous Reversible Deactivation Radical Polymerization. *Acta Polym. Sin.* **2023**, 54 (6), 761–777.
- (9) Chen, M.; Zhong, M.; Johnson, J. A. Light-Controlled Radical Polymerization: Mechanisms, Methods, and Applications. *Chem. Rev.* **2016**, *116* (17), 10167–10211.
- (10) Wang, J.-S.; Matyjaszewski, K. Controlled/living Radical Polymerization. Atom Transfer Radical Polymerization in the Presence of Transition-Metal Complexes. J. Am. Chem. Soc. 1995, 117 (20), 5614–5615.
- (11) Chiefari, J.; Chong, Y. K.; Ercole, F.; Krstina, J.; Jeffery, J.; Le, T. P. T.; Mayadunne, R. T. A.; Meijs, G. F.; Moad, C. L.; Moad, G.; Rizzardo, E.; Thang, S. H.; Thang, S. H. Living Free-Radical Polymerization by Reversible Addition—Fragmentation Chain Transfer: The RAFT Process. *Macromolecules* 1998, 31 (16), 5559—5562.
- (12) Lorandi, F.; Fantin, M.; Matyjaszewski, K. Atom Transfer Radical Polymerization: A Mechanistic Perspective. *J. Am. Chem. Soc.* **2022**, *144* (34), 15413–15430.
- (13) Moad, G.; Rizzardo, E.; Thang, S. H. Living Radical Polymerization by the RAFT Process. *Aust. J. Chem.* **2005**, *58* (6), 379–410.
- (14) Stenzel, M. H.; Barner-Kowollik, C. The Living Dead Common Misconceptions about Reversible Deactivation Radical Polymerization. *Mater. Horiz.* **2016**, 3 (6), 471–477.
- (15) Chong, Y. K.; Le, T. P. T.; Moad, G.; Rizzardo, E.; Thang, S. H. A More Versatile Route to Block Copolymers and Other Polymers of Complex Architecture by Living Radical Polymerization: The RAFT Process. *Macromolecules* **1999**, 32 (6), 2071–2074.
- (16) Mühlebach, A.; Gaynor, S. G.; Matyjaszewski, K. Synthesis of Amphiphilic Block Copolymers by Atom Transfer Radical Polymerization (ATRP). *Macromolecules* **1998**, *31* (18), 6046–6052.
- (17) Pearson, S.; St Thomas, C.; Guerrero-Santos, R.; D'Agosto, F. Opportunities for Dual RDRP Agents in Synthesizing Novel Polymeric Materials. *Polym. Chem.* **2017**, 8 (34), 4916–4946.
- (18) Corrigan, N.; Boyer, C. 100th Anniversary of Macromolecular Science Viewpoint: Photochemical Reaction Orthogonality in Modern Macromolecular Science. *ACS Macro Lett.* **2019**, 8 (7), 812–818.
- (19) Xu, J.; Shanmugam, S.; Fu, C.; Aguey-Zinsou, K.-F.; Boyer, C. Selective Photoactivation: From a Single Unit Monomer Insertion Reaction to Controlled Polymer Architectures. *J. Am. Chem. Soc.* **2016**, 138 (9), 3094–3106.
- (20) Tanaka, J.; Häkkinen, S.; Boeck, P. T.; Cong, Y.; Perrier, S.; Sheiko, S. S.; You, W. Orthogonal Cationic and Radical RAFT Polymerizations to Prepare Bottlebrush Polymers. *Angew. Chem., Int. Ed.* **2020**, *59* (18), 7203–7208.

- (21) Shanmugam, S.; Cuthbert, J.; Kowalewski, T.; Boyer, C.; Matyjaszewski, K. Catalyst-Free Selective Photoactivation of RAFT Polymerization: A Facile Route for Preparation of Comblike and Bottlebrush Polymers. *Macromolecules* **2018**, *51* (19), 7776–7784.
- (22) Corrigan, N.; Trujillo, F. J.; Xu, J.; Moad, G.; Hawker, C. J.; Boyer, C. Divergent Synthesis of Graft and Branched Copolymers through Spatially Controlled Photopolymerization in Flow Reactors. *Macromolecules* **2021**, 54 (7), 3430–3446.
- (23) Shanmugam, S.; Cuthbert, J.; Flum, J.; Fantin, M.; Boyer, C.; Kowalewski, T.; Matyjaszewski, K. Transformation of Gels via Catalyst-Free Selective RAFT Photoactivation. *Polym. Chem.* **2019**, *10* (19), 2477–2483.
- (24) Yang, S.; Zhang, L.; Chen, Y.; Tan, J. Combining Green Light-Activated Photoiniferter RAFT Polymerization and RAFT Dispersion Polymerization for Graft Copolymer Assemblies. *Macromolecules* **2022**, 55 (19), 8472–8484.
- (25) Nicolaÿ, R.; Kwak, Y.; Matyjaszewski, K. Dibromotrithiocarbonate Iniferter for Concurrent ATRP and RAFT Polymerization. Effect of Monomer, Catalyst, and Chain Transfer Agent Structure on the Polymerization Mechanism. *Macromolecules* **2008**, *41* (13), 4585–4596.
- (26) Bolton, J.; Rzayev, J. Tandem RAFT-ATRP Synthesis of Polystyrene-Poly(Methyl Methacrylate) Bottlebrush Block Copolymers and Their Self-Assembly into Cylindrical Nanostructures. *ACS Macro Lett.* **2012**, *1* (1), 15–18.
- (27) Lin, Z.; Sang, Y.; Nie, Z. Stepwise Self-Assembly of Bottlebrush Random Copolymers into Uniform Cylindrical Structures. *Colloid Polym. Sci.* **2023**, *301* (9), 1021–1028.
- (28) Li, F.; Cao, M.; Feng, Y.; Liang, R.; Fu, X.; Zhong, M. Site-Specifically Initiated Controlled/Living Branching Radical Polymerization: A Synthetic Route toward Hierarchically Branched Architectures. J. Am. Chem. Soc. 2019, 141 (2), 794–799.
- (29) Li, Z.; Tang, M.; Liang, S.; Zhang, M.; Biesold, G. M.; He, Y.; Hao, S.-M.; Choi, W.; Liu, Y.; Peng, J.; Lin, Z. Bottlebrush Polymers: From Controlled Synthesis, Self-Assembly, Properties to Applications. *Prog. Polym. Sci.* **2021**, *116*, 101387.
- (30) Xie, G.; Martinez, M. R.; Olszewski, M.; Sheiko, S. S.; Matyjaszewski, K. Molecular Bottlebrushes as Novel Materials. *Biomacromolecules* **2019**, 20 (1), 27–54.
- (31) Li, Y.; Li, Y.; Yan, R.; Zhang, L.; Liu, H.; Tan, J. Chain Architecture as an Orthogonal Parameter to Tune Morphologies of Polymer Assemblies: Efficient Synthesis and Self-Assembly of Linear-Branched Block Copolymers via RAFT Dispersion Polymerization. *Macromolecules* **2024**, *57* (11), 5175–5188.
- (32) Lin, W.; Jia, S.; Li, Y.; Zhang, L.; Liu, H.; Tan, J. Aqueous RAFT Dispersion Polymerization Mediated by an ω,ω-Macromolecular Chain Transfer Monomer: An Efficient Approach for Amphiphilic Branched Block Copolymers and the Assemblies. *ACS Macro Lett.* **2024**, *13*, 1022–1030.
- (33) Zhao, S.; Zhang, L.; Tan, J. In Situ Synthesis of Branched Block Copolymer Assemblies via RAFT Dispersion Polymerization Using Branched Macro-RAFT Agents. *Chin. J. Chem.* **2023**, *41* (12), 1517–1525.
- (34) Cai, W.; Yang, S.; Zhang, L.; Chen, Y.; Zhang, L.; Tan, J. Efficient Synthesis and Self-Assembly of Segmented Hyperbranched Block Copolymers via RAFT-Mediated Dispersion Polymerization Using Segmented Hyperbranched Macro-RAFT Agents. *Macromolecules* **2022**, 55 (13), 5775–5787.
- (35) Luo, X.; Zhang, K.; Zeng, R.; Chen, Y.; Zhang, L.; Tan, J. Segmented Copolymers Synthesized by Reversible Addition-Fragmentation Chain Transfer (RAFT) Polymerization Using an Asymmetric Difunctional RAFT Agent and the Utilization in RAFT-Mediated Dispersion Polymerization. *Macromolecules* **2022**, *55* (1), 65–77.
- (36) Hou, W.; Li, Z.; Xu, L.; Li, Y.; Shi, Y.; Chen, Y. High-Yield Synthesis of Molecular Bottlebrushes via PISA-Assisted Grafting-from Strategy. ACS Macro Lett. 2021, 10 (10), 1260–1265.
- (37) Lin, W.; Jia, S.; Li, Y.; Zhang, L.; Liu, H.; Tan, J. Aqueous RAFT Dispersion Polymerization Mediated by an ω,ω-Macromolecular Chain Transfer Monomer: An Efficient Approach for Amphiphilic

- Branched Block Copolymers and the Assemblies. ACS Macro Lett. 2024, 13 (8), 1022-1030.
- (38) Xie, G.; Wu, J.; Zhang, L.; Tan, J. Efficient Synthesis of  $\mu$ -A(BC)C Miktoarm Star Polymer Assemblies via Aqueous Photo-initiated Polymerization-Induced Self-Assembly. *Langmuir* **2024**, *40* (32), 17098–17108.
- (39) Han, S.; Wu, J.; Zhang, Y.; Lai, J.; Chen, Y.; Zhang, L.; Tan, J. Utilization of Poor RAFT Control in Heterogeneous RAFT Polymerization. *Macromolecules* **2021**, *54* (10), 4669–4681.
- (40) Wu, J.; Zhang, L.; Chen, Y.; Tan, J. Linear and Star Block Copolymer Nanoparticles Prepared by Heterogeneous RAFT Polymerization Using an ω,ω-Heterodifunctional Macro-RAFT Agent. ACS Macro Lett. 2022, 11 (7), 910–918.
- (41) Xu, J.; Jung, K.; Atme, A.; Shanmugam, S.; Boyer, C. A Robust and Versatile Photoinduced Living Polymerization of Conjugated and Unconjugated Monomers and Its Oxygen Tolerance. *J. Am. Chem. Soc.* **2014**, *136* (14), 5508–5519.
- (42) Lai, J. T.; Filla, D.; Shea, R. Functional Polymers from Novel Carboxyl-Terminated Trithiocarbonates as Highly Efficient RAFT Agents. *Macromolecules* **2002**, 35 (18), 6754–6756.
- (43) Pacheco, A. A. C.; da Silva Filho, A. F.; Kortsen, K.; Hanson-Heine, M. W. D.; Taresco, V.; Hirst, J. D.; Lansalot, M.; D'Agosto, F.; Howdle, S. M. Influence of Structure and Solubility of Chain Transfer Agents on the RAFT Control of Dispersion Polymerisation in scCO2. *Chem. Sci.* 2021, 12 (3), 1016–1030.
- (44) Moad, G.; Chong, Y. K.; Postma, A.; Rizzardo, E.; Thang, S. H. Advances in RAFT Polymerization: The Synthesis of Polymers with Defined End-Groups. *Polymer* **2005**, *46* (19), 8458–8468.
- (45) Gody, G.; Zetterlund, P. B.; Perrier, S.; Harrisson, S. The Limits of Precision Monomer Placement in Chain Growth Polymerization. *Nat. Commun.* **2016**, *7* (1), 10514.
- (46) Warren, N. J.; Armes, S. P. Polymerization-Induced Self-Assembly of Block Copolymer Nano-Objects via RAFT Aqueous Dispersion Polymerization. *J. Am. Chem. Soc.* **2014**, *136* (29), 10174–10185.
- (47) Canning, S. L.; Smith, G. N.; Armes, S. P. A Critical Appraisal of RAFT-Mediated Polymerization-Induced Self-Assembly. *Macromolecules* **2016**, 49 (6), 1985–2001.
- (48) Penfold, N. J. W.; Yeow, J.; Boyer, C.; Armes, S. P. Emerging Trends in Polymerization-Induced Self-Assembly. ACS Macro Lett. **2019**, 8 (8), 1029–1054.
- (49) Liu, C.; Hong, C.-Y.; Pan, C.-Y. Polymerization Techniques in Polymerization-Induced Self-Assembly (PISA). *Polym. Chem.* **2020**, *11* (22), 3673–3689.
- (50) Zhang, W.-J.; Hong, C.-Y.; Pan, C.-Y. Polymerization-Induced Self-Assembly of Functionalized Block Copolymer Nanoparticles and Their Application in Drug Delivery. *Macromol. Rapid Commun.* **2019**, 40 (2), 1800279.
- (51) Li, S.; Han, G.; Zhang, W. Cross-Linking Approaches for Block Copolymer Nano-Assemblies via RAFT-Mediated Polymerization-Induced Self-Assembly. *Polym. Chem.* **2020**, *11* (29), 4681–4692.
- (52) Bowman, J. I.; Eades, C. B.; Vratsanos, M. A.; Gianneschi, N. C.; Sumerlin, B. S. Ultrafast Xanthate-Mediated Photoiniferter Polymerization-Induced Self-Assembly (PISA). *Angew. Chem., Int. Ed.* **2023**, 62 (48), No. e202309951.
- (53) Rho, J. Y.; Scheutz, G. M.; Häkkinen, S.; Garrison, J. B.; Song, Q.; Yang, J.; Richardson, R.; Perrier, S.; Sumerlin, B. S. In Situ Monitoring of PISA Morphologies. *Polym. Chem.* **2021**, *12* (27), 3947–3952.
- (54) Touve, M. A.; Figg, C. A.; Wright, D. B.; Park, C.; Cantlon, J.; Sumerlin, B. S.; Gianneschi, N. C. Polymerization-Induced Self-Assembly of Micelles Observed by Liquid Cell Transmission Electron Microscopy. *ACS Cent. Sci.* **2018**, *4* (5), 543–547.
- (55) Sun, H.; Cao, W.; Zang, N.; Clemons, T. D.; Scheutz, G. M.; Hu, Z.; Thompson, M. P.; Liang, Y.; Vratsanos, M.; Zhou, X.; Choi, W.; Sumerlin, B. S.; Stupp, S. I.; Gianneschi, N. C. Proapoptotic Peptide Brush Polymer Nanoparticles via Photoinitiated Polymerization-Induced Self-Assembly. *Angew. Chem., Int. Ed.* **2020**, *59* (43), 19136–19142.

- (56) Luo, X.; An, Z. Polymerization-Induced Self-Assembly for the Preparation of Poly(N,N-dimethylacrylamide)-b(4-tert-butoxystyrene-co-pentafluorostyrene) Particles with Inverse Bicontinuous Phases<sup>†</sup>. *Chin. J. Chem.* **2021**, 39 (7), 1819–1824.
- (57) Wang, X.; Shen, L.; An, Z. Dispersion Polymerization in Environmentally Benign Solvents via Reversible Deactivation Radical Polymerization. *Prog. Polym. Sci.* **2018**, 83, 1–27.
- (58) Yeow, J.; Boyer, C. Photoinitiated Polymerization-Induced Self-Assembly (Photo-PISA): New Insights and Opportunities. *Adv. Sci.* **2017**, *4* (7), 1700137.
- (59) He, J.; Chen, Y.; Zhang, L.; Tan, J. Oxidation-Responsive Framboidal Triblock Copolymer Vesicles Prepared by Photoinitiated RAFT Seeded Emulsion Polymerization. *Chin. Chem. Lett.* **2023**, 34 (3), 107344.
- (60) Hou, W.; Yin, X.; Zhou, Y.; Zhou, Z.; Liu, Z.; Du, J.; Shi, Y.; Chen, Y. Kinetically Controlled Preparation of Worm-like Micelles with Tunable Diameter/Length and Structural Stability. *J. Am. Chem. Soc.* **2024**, *146* (34), 24094–24104.
- (61) Wang, X.; Figg, C. A.; Lv, X.; Yang, Y.; Sumerlin, B. S.; An, Z. Star Architecture Promoting Morphological Transitions during Polymerization-Induced Self-Assembly. *ACS Macro Lett.* **2017**, *6* (4), 337–342.
- (62) Zhang, X.; Wei, Z.; Liu, K.; Wang, L.; Yang, W. A3B-Type Miktoarm Star Polymer Nanoassemblies Prepared by Reversible Addition—Fragmentation Chain Transfer (RAFT) Dispersion Polymerization. *Polym. Chem.* **2022**, *13* (38), 5494—5506.
- (63) Wang, R.; Zhu, W.; Zhang, L.; Sheng, X.; Tan, J. Synthesis of Self-Assembled Star/Linear Block Copolymer Blends via Aqueous RAFT Dispersion Polymerization. *Chin. J. Chem.* **2024**, 42 (14), 1606–1614.
- (64) Zeng, R.; Chen, Y.; Zhang, L.; Tan, J. R-RAFT or Z-RAFT? Well-Defined Star Block Copolymer Nano-Objects Prepared by RAFT-Mediated Polymerization-Induced Self-Assembly. *Macromolecules* **2020**, 53 (5), 1557–1566.
- (65) Zhang, Y.; Cao, M.; Han, G.; Guo, T.; Ying, T.; Zhang, W. Topology Affecting Block Copolymer Nanoassemblies: Linear Block Copolymers versus Star Block Copolymers under PISA Conditions. *Macromolecules* **2018**, *51* (14), 5440–5449.
- (66) Hou, W.; Wu, J.; Li, Z.; Zhang, Z.; Shi, Y.; Chen, Y. Efficient Synthesis and PISA Behavior of Molecular Bottlebrush Block Copolymers via a Grafting-From Strategy through RAFT Dispersion Polymerization. *Macromolecules* **2023**, *56* (3), 824–832.